A Versatile Strategy for the Preparation of Woody Biochar with Oxygen-rich Groups and Enhanced Porosity for Highly Efficient Cr(VI) Removal

Hongping Dong [a,b,c], Lin Zhang [a,b,c,*], Lishu Shao [a,b,c], Zhiping Wu [a,b,c], Peng Zhan [a,b,c], Xiaoxun Zhou [d], Jienan Chen [a,b,c,*]

[a] *College of Materials Science and Engineering, Central South University of Forestry and Technology, Changsha 410004, China*

[b] *Ministry of Forestry Bioethanol Research Center, Changsha 410004, China*

[c] *Hunan International Joint Laboratory of Woody Biomass Conversion, Changsha 410004, China*

[d] *College of Hoticulture, Hunan Agricultural University, Changsha,410128,China*

*Corresponding author: Jienan Chen, E-mail: chenjnx@163.com; Lin Zhang, E-mail: zhlin-331@163.com

S1. Calculation of Cellulose, hemicellulose, and lignin contents

The yield (Y) was calculated as:

$$\text{Yield}=(\frac{m_1}{m_2})\times 100\% \quad (1)$$

Where m_2 is the weight of DW sample, m_1 is the weight of dry PW sample.

The normalized value of content for cellulose, hemicellulose and lignin are calculated as:

$$C_{norm} = (C_{test} \times Y) \times 100\% \quad (2)$$

where C_{test} is the test value of cellulose (or hemicellulose, or lignin) content, Y refers to the yield, and C_{norm} is the normalized value of cellulose (or hemicellulose, or lignin) content. All the test and normalized values of cellulose, hemicellulose, and lignin for the four samples are summarized in Table S1.

S2. Batch experiments

The pseudo-first-order kinetic model and pseudo-second-order kinetic model were used to evaluate the fitting data based on the equations as follows:

Pseudo-first-order kinetic model equation:

$$q_t = q_e[1-\exp(-k_1 t)] \quad (3)$$

Pseudo-second-order kinetic model equation:

$$q_t = \frac{q_e^2 k_2 t}{(1+q_e k_2 t)} \quad (4)$$

Where q_t and q_e (mg g^{-1}) are the adsorption capacity at time t and the equilibrium adsorption capacity, respectively; t (min) is the adsorption time; k_1 (min^{-1}) and k_2 (g mg^{-1} min^{-1}) represent the rate constant of the pseudo-first-order kinetic model and the

pseudo-second-order kinetic model, respectively.

Langmuir (Eq. 5) and Freundlich model (Eq. 6) were used to fit the isothermal adsorption curves of biochar. The free energy change (ΔG, kJ mol^{-1}), heat of adsorption (ΔH, kJ mol^{-1}) and change in adsorption entropy (ΔS, kJ $mol^{-1}\cdot K^{-1}$) of the adsorption process are also calculated. The formulas are as follows:

Langmuir model equation:

$$q_e = \frac{kq_{\max}c_e}{(1+kc_e)} \tag{5}$$

Freundlich model equation:

$$q_e = k_f c_e^{\frac{1}{n}} \tag{6}$$

Thermodynamic formula:

$$\Delta G = -RT\ln k_a \tag{7}$$

$$\Delta G = \Delta H - T\Delta S \tag{8}$$

$$\ln k_a = \frac{\Delta S}{R} - \frac{\Delta H}{RT} \tag{9}$$

where q_e and $q_{\max}$ (mg g^{-1}) are the equilibrium adsorption capacity and the maximum adsorption capacity, respectively; k is the Langmuir constant; C_e (mg L^{-1}) is the concentration of Cr(VI) in solution at the adsorption equilibrium; k_f and n refers to the Freundlich constants; R (8.314 J $mol^{-1}\cdot K^{-1}$) and k_a represent the universal gas constant and the Langmuir constant(k); T (K) is the experimental temperature.

The equation of the intra-particle diffusion model is as follows:

$$q_t = k_i t^{0.5} + C \tag{10}$$

where q_t (mg g^{-1}) is the adsorption capacity at time t; K_i (mg $g^{-1}\cdot min^{0.5}$) and C are the

intraparticle diffusion rate constant and the model constant, respectively.

S3. DFT calculations

Based on the previous research, the electron density distribution of the as-prepared ACDW in solution was calculated by DFT in which a simple graphite structure with seven aromatic rings was used as the aromatic carbon structure, and the functional groups of phenolic hydroxyl, carboxyl, lactone, ether and semiquinone were modified on the surface, respectively. No special processing was done on the core electronics, all electrons participated in the calculation of the system, and the core treatment was set to "All Electrons". The electronic base set was DND3.5. The SCF (self-consistent field convergence) value was 1×10^{-5}. The COSMO (conduct or like screening model) solvation calculation of the periodic model was performed. The solvent was water and the dielectric constant was 78.54 (298 K, 101.325 kPa). The exchange correlation function was GGA (General gradient-corrected) PBE (Perdew, Burke and Enzerhof).

S4. Figures

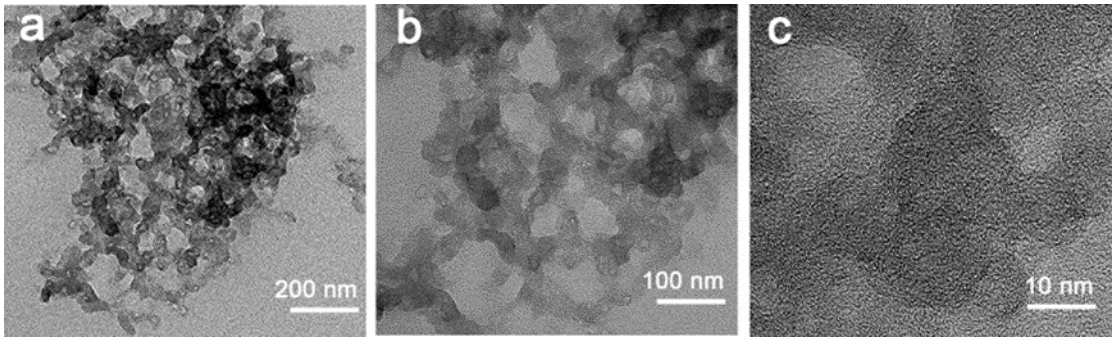

Figure S1 TEM images of ACDW at low (a) and high (b, c) resolution.

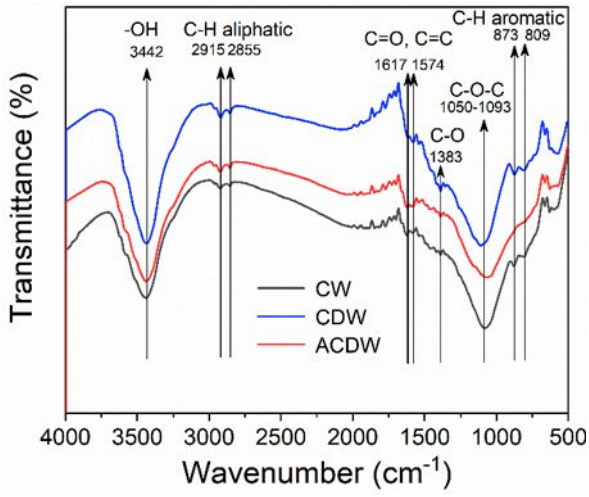

Figure S2 The FT-IR spectra of CW, CDW and ACDW.

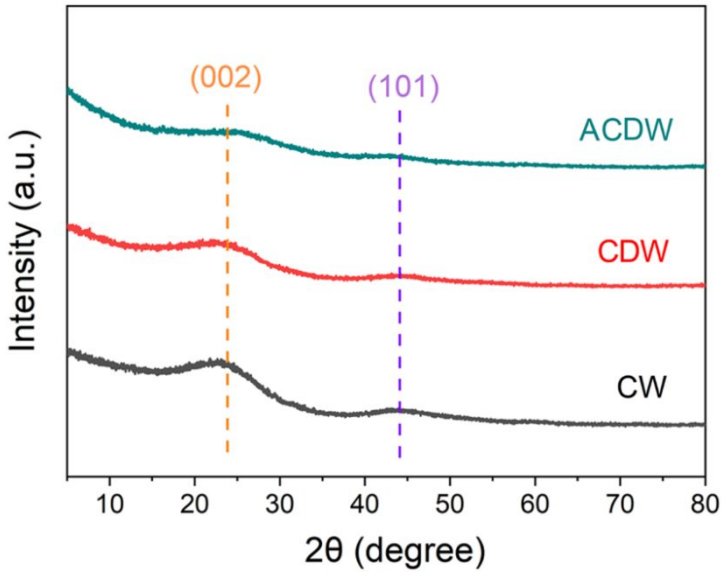

Figure S3 XRD patterns of CW, CDW and ACDW.

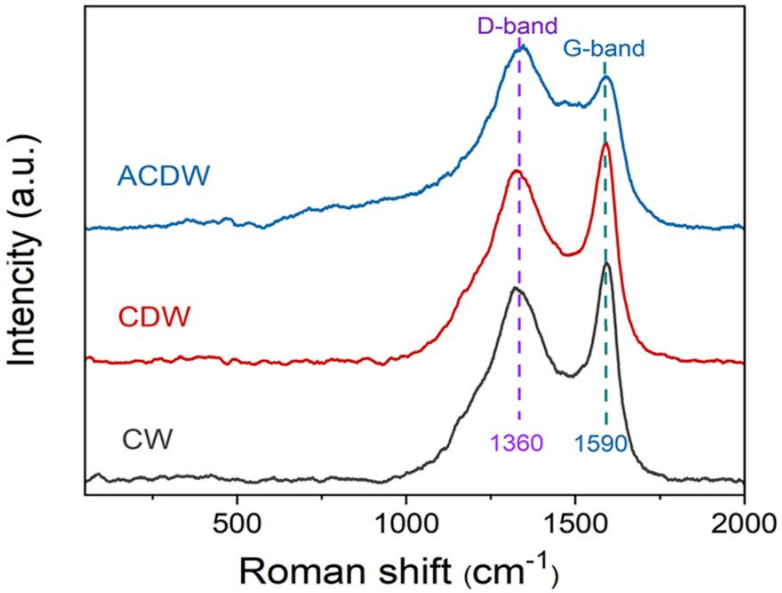

Figure S4 Raman spectra of CW, CDW and ACDW.

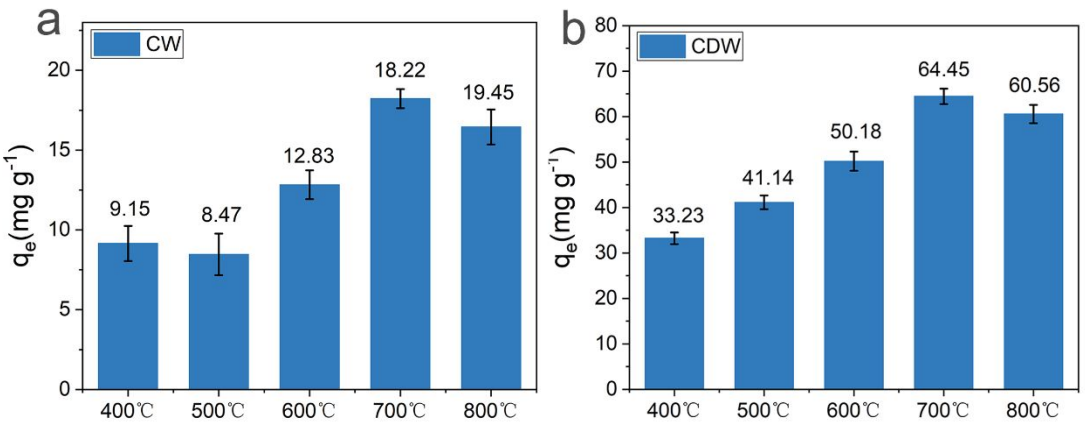

Figure S5 The effect of different carbonization temperatures on the Cr adsorption capacity of CW (a) and CDW (b).

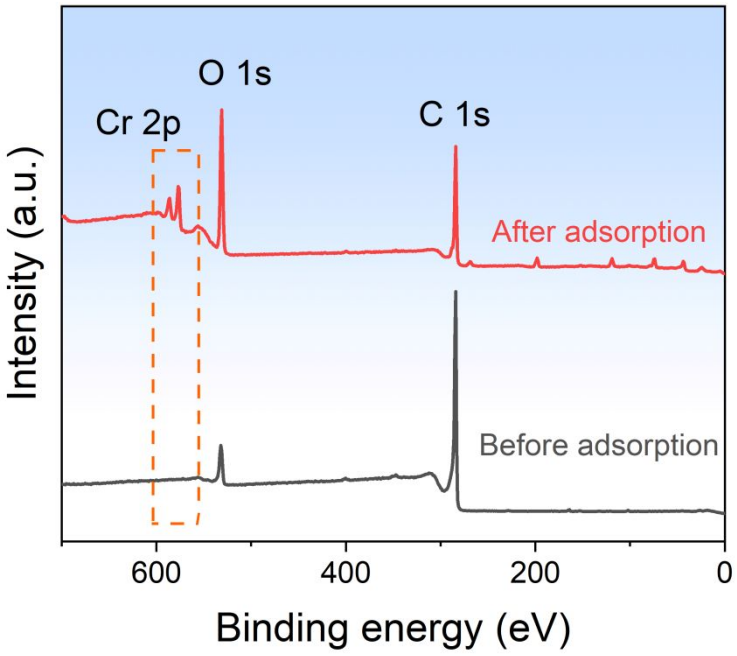

Figure S6 The XPS survey spectra of ACDW before and after Cr adsorption.

S5. Tables

Table S1 The evolution of chemical components from PW to DW.

Sample	Parameter	Cellulose (%)	Hemicellulose (%)	Lignin (%)
PW	Test value#	42.36	14.56	28.75
DW	Test value	63.08	14.43	12.06
	Yield		53%	
	After normalization	33.43 (63.08×53%)	7.65 (14.43×53%)	6.39 (12.06×53%)

#. As the yield value of PW is 100%, the normalization value is equal to the test value.

Table S2 Porosity parameters of CW, CDW and ACDW calculated from nitrogen adsorption-desorption isotherm.

Material	S_{BET} ($m^2\ g^{-1}$)	V_{tot} ($cm^3\ g^{-1}$)	V_{mi} ($cm^3\ g^{-1}$)	V_{me} ($cm^3\ g^{-1}$)	D (nm)
CW	57.3	0.145	0.008	0.137	9.59
CDW	236.4	0.290	0.036	0.254	6.36
ACDW	970.9	1.030	0.146	0.884	5.75

S_{BET}: BET specific surface area; V_{tot}: total pore volume; V_{mi}: micropore volume; V_{me}: mesopore volume; D: average pore diameter.

Table S3 Adsorption Kinetics parameters of ACDW

Model name	Model related parameters		
	k	q_e (mg g^{-1})	R^2
Pseudo-first order	0.053	173.45	0.72
Pseudo-second order	6.83×10^{-4}	178.92	0.96

Table S4 Isothermal adsorption parameters, calculated based on Eq.S5−6.

T (k)	$q_{max,exp}$ (mg g^{-1})	Langmuir model			Freundlich model		
		q_{max} (mg g^{-1})	K (L mg g^{-1})	R^2	k_f(mg g^{-1})	n	R^2
298	297.5	294.86	4.92	0.96	252.02	28.57	0.77
308	308	301.72	11.25	0.97	264.08	31.83	0.78
318	318.6	307.76	16.87	0.95	291.89	38.46	0.74

Table S5 Comparison of removal adsorption capacity of Cr(VI) on various adsorbents in their optimum conditions.

Raw material	Activator	S_{BET} (m^2 g^{-1})	q_{max} (mg g^{-1})	Adsorption per unit area (mg m^2)	Ref.
Peanut hull	$FeCl_3$	145.25	77.54	0.53	1
Bagasse	$ZnCl_2$	916.13	80.88	0.09	2
Wood apple shell	H_2SO_4	1898.00	151.51	0.08	3
Glucose	KOH	1491.21	230.15	0.15	4
Fox nutshell	$ZnCl_2$	2869.00	46.21	0.02	5
Corn straw	KOH	2183.80	116.97	0.05	6
Corn straw	KOH	2131.18	175.44	0.08	7
Poplar wood sawdust	KOH	970.52	294.86	0.30	This work

Table S6 Thermodynamic parameters for the adsorption of ACDW, calculated based on Eq. S7–9.

T (K)	k_a (L mol^{-1})	ΔG (kJ mol^{-1})	ΔH (kJ mol^{-1})	ΔS (kJ K^{-1} mol^{-1})
298	4.92×10^3	-21.620		
308	11.25×10^3	-23.886	48.703	0.235
318	16.87×10^3	-25.733		

Table S7 Parameters of intraparticle diffusion model.

Initial concentration of Cr(VI) (mg g^{-1})	40 mg	60 mg	100 mg	150 mg	200 mg
$k_{i,1}$	0.966	3.438	3.561	3.202	4.637
C_1	107.42	126.13	145	161.23	173.6
R_1^2	0.924	0.977	0.98	0.969	0.963
$k_{i,2}$	0.023	0.487	1.558	1.301	0.83
C_2	119.53	164.86	183.4	188.83	223.66
R_2^2	0.709	0.963	0.96	0.99	0.91

Reference

1. Han, Y.; Cao, X.; Ouyang, X.; Sohi, S. P.; Chen, J., Adsorption kinetics of magnetic biochar derived from peanut hull on removal of Cr (VI) from aqueous solution: Effects of production conditions and particle size. *Chemosphere* **2016,** 145, 336-41.

2. Zeng, X. L. Y. C. L. L. J., Cr(VI) adsorption performance and mechanism of an effective activated carbon prepared from bagasse with a one-step pyrolysis and $ZnCl_2$ activation method. *Cellulose* **2019,** 26, 4921-4934.

3. Doke, K. M.; Khan, E. M., Equilibrium, kinetic and diffusion mechanism of Cr(VI) adsorption onto activated carbon derived from wood apple shell. *Arab. J. Chem.* **2017,** 10, S252-S260.

4. Xu, H.; Liu, Y.; Liang, H.; Gao, C.; Qin, J.; You, L.; Wang, R.; Li, J.; Yang, S., Adsorption of Cr(VI) from aqueous solutions using novel activated carbon spheres derived from glucose and sodium dodecylbenzene sulfonate. *Sci. Total Environ.* **2021,** 759, 143457.

5. Kumar, A.; Jena, H. M., Adsorption of Cr(VI) from aqueous phase by high surface area activated carbon prepared by chemical activation with $ZnCl_2$. *Process Saf Environ Prot* **2017,** 109, 63-71.

6. Qu, J.; Wang, Y.; Tian, X.; Jiang, Z.; Deng, F.; Tao, Y.; Jiang, Q.; Wang, L.; Zhang, Y., KOH-activated porous biochar with high specific surface area for adsorptive removal of chromium (VI) and naphthalene from water: Affecting factors, mechanisms and reusability exploration. *J. Hazard. Mater.* **2021,** 401, 123292.

7. Ma, H.; Yang, J.; Gao, X.; Liu, Z.; Liu, X.; Xu, Z., Removal of chromium (VI) from

water by porous carbon derived from corn straw: Influencing factors, regeneration and mechanism. *J. Hazard. Mater.* **2019,** 369, 550-560.